



5-2004

## Combined Mutual Information of Intensity and Gradient for Multi-modal Medical Image Registration

Wei Jiang  
*University of Tennessee, Knoxville*

Follow this and additional works at: [https://trace.tennessee.edu/utk\\_gradthes](https://trace.tennessee.edu/utk_gradthes)



Part of the [Electrical and Computer Engineering Commons](#)

---

### Recommended Citation

Jiang, Wei, "Combined Mutual Information of Intensity and Gradient for Multi-modal Medical Image Registration. " Master's Thesis, University of Tennessee, 2004.  
[https://trace.tennessee.edu/utk\\_gradthes/4630](https://trace.tennessee.edu/utk_gradthes/4630)

This Thesis is brought to you for free and open access by the Graduate School at TRACE: Tennessee Research and Creative Exchange. It has been accepted for inclusion in Masters Theses by an authorized administrator of TRACE: Tennessee Research and Creative Exchange. For more information, please contact [trace@utk.edu](mailto:trace@utk.edu).

To the Graduate Council:

I am submitting herewith a thesis written by Wei Jiang entitled "Combined Mutual Information of Intensity and Gradient for Multi-modal Medical Image Registration." I have examined the final electronic copy of this thesis for form and content and recommend that it be accepted in partial fulfillment of the requirements for the degree of Master of Science, with a major in Electrical Engineering.

Seong G. Kong, Major Professor

We have read this thesis and recommend its acceptance:

Mongi A. Abidi, Hairong Qi

Accepted for the Council:

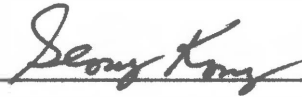
Carolyn R. Hodges

Vice Provost and Dean of the Graduate School

(Original signatures are on file with official student records.)

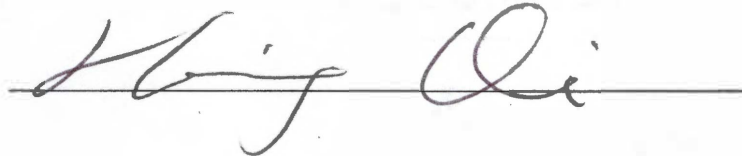
To the Graduate Council:

I am submitting herewith a thesis written by Wei Jiang entitled "Combined Mutual Information of Intensity and Gradient for Multi-modal Medical Image Registration". I have examined the final paper copy of this thesis for form and content and recommend that it be accepted in partial fulfillment of the requirements for the degree of Master of Science, with a major in Electrical Engineering.

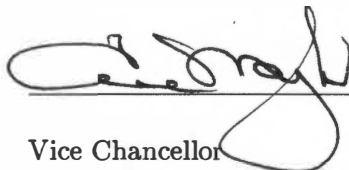


Dr. Seong G. Kong, Major Professor

We have read this thesis  
and recommend its acceptance:



Accepted for the Council:



Vice Chancellor  
and Dean of Graduate Studies

Thesis  
2004  
.J53

1-53 2004  
J53 .J53

1-53 2004  
J53 .J53

1-53 2004  
J53 .J53

**COMBINED MUTUAL INFORMATION OF  
INTENSITY AND GRADIENT FOR MULTI-MODAL  
MEDICAL IMAGE REGISTRATION**

A Thesis

Presented for the

Master of Science Degree

The University of Tennessee, Knoxville

Wei Jiang

May 2004

## **Acknowledgments**

I would like to express my deepest gratitude to my advisor Dr. Seong G. Kong for his excellent academic guidance. His high standard has challenged me to excel, while his encouragement and support make it possible for me to finish this thesis. I am very thankful for the support and encouragement of my other Thesis Committee members, Dr. Mongi A. Abidi and Dr. Hairong Qi.

I would like to thank Dr. Jeffrey T. Yap of University of Tennessee Medical Center who provided us the image data used in the thesis and offered excellent advice with technical aspects. Also, I received generous financial support from the Department of Electrical and Computer Engineering.

My thanks go to my wife, Lidan Miao, and my parents for their endless love and support.

## Abstract

In this thesis, registration methods for multi-modal medical images are reviewed with mutual information-based methods discussed in detail. Since it was proposed, mutual information has gained intensive research and is getting very popular, however its robustness is questionable and may fail in some cases. The possible reason might be it does not consider the spatial information in the image pair. In order to improve this measure, the thesis proposes to use combined mutual information of intensity and gradient for multi-modal medical image registration. The proposed measure utilizes both the intensity and gradient information of an image pair. Maximization of this measure is assumed to correctly register an image pair. Optimization of the registration measure in a multi-dimensional space is another major issue in multi-modal medical image registration. The thesis first briefly reviews the commonly used optimization techniques and then discusses in detail the Powell's conjugate direction set method, which is implemented to find the maximum of the combined mutual information of an image pair. In the experiment, we first register slice images scanned in a single patient in the same or different scanning sessions by the proposed method. Then 20 pairs of co-registered CT and PET slice images at three different resolutions are used to study the performance of the proposed measure and four other measures discussed in this thesis. Experimental results indicate that the proposed combined measure produces reliable registrations and it outperforms the intensity- and gradient-based measures at all three resolutions.

# Contents

<b>1</b>	<b>Introduction</b>	<b>1</b>
1.1	Background . . . . .	1
1.2	Concept of Image Registration . . . . .	2
1.3	State of the Art . . . . .	4
1.4	Thesis Goal and Outline . . . . .	6
<b>2</b>	<b>Literature Review</b>	<b>8</b>
2.1	Overview . . . . .	8
2.2	Registration Methods for Multi-modal Medical Images . . . . .	9
2.2.1	Extrinsic Methods . . . . .	9
2.2.2	Intrinsic Methods . . . . .	11
2.3	Summary . . . . .	15
<b>3</b>	<b>Image Registration by Mutual Information</b>	<b>17</b>
3.1	Definitions . . . . .	17
3.2	Mutual Information of Intensity . . . . .	20



3.3	Mutual Information of Gradient . . . . .	22
3.4	Combined Mutual Information for Image Registration . . . . .	26
3.5	Transformation Model . . . . .	30
3.6	Mutual Information Weighed by Gradient Term . . . . .	31
3.7	Multiplication of Intensity- and Gradient-based Mutual Information . . . . .	33
<b>4</b>	<b>Optimization of Registration Measure</b>	<b>34</b>
4.1	Problem Statement . . . . .	34
4.2	Overview of Optimization Methods . . . . .	36
4.3	Multi-dimensional Optimization . . . . .	37
4.3.1	Conjugate Directions . . . . .	38
4.3.2	Powell's Method . . . . .	39
4.3.3	Golden Section Search . . . . .	40
<b>5</b>	<b>Experiment Results</b>	<b>43</b>
5.1	Dataset Description . . . . .	43
5.2	Registration Error Estimation . . . . .	46
5.3	Registration Result . . . . .	49
5.3.1	Mosaic Images . . . . .	49
5.3.2	Registration Accuracy Study . . . . .	51
5.3.3	Registration Robustness Study . . . . .	52
5.4	Summary . . . . .	56

<b>6 Conclusion</b>	<b>58</b>
<b>Bibliography</b>	<b>61</b>
<b>Vita</b>	<b>71</b>

# List of Tables

5.1	Description of dataset one . . . . .	44
5.2	Description of dataset two . . . . .	45
5.3	Description of dataset three . . . . .	45
5.4	Registration error for accuracy study (In mm) . . . . .	52
5.5	Registration error for robustness study (In mm) . . . . .	55

# List of Figures

1.1	A pair of multi-modal medical images. . . . .	4
3.1	Joint PDF and corresponding joint entropy values of an image pair before and after registration. . . . .	21
3.2	A synthetic example where the intensity mutual information successfully registers the images. . . . .	21
3.3	Illustration of the limitation of the intensity mutual information . . . . .	23
3.4	Gradient magnitude of a pair of CT and PET images . . . . .	24
3.5	Registration function of the two images in Fig. 3.3 . . . . .	25
3.6	CT-PET image registration by the proposed combined mutual information. 27	
4.1	Golden section search for 1D optimization . . . . .	41
5.1	Calculation of the mean displacement . . . . .	48
5.2	Two pairs of CT/PET images from the first dataset and registration result by the combined mutual information . . . . .	50

5.3	Two pairs of CT/PET images from the second dataset and registration result by the combined mutual information . . . . .	50
5.4	Two pairs of CT/PET images from the third dataset and registration result by the combined mutual information . . . . .	50
5.5	Mean displacements of $I$ , $I_g$ and $I_c$ for 20 image pairs at 8mm resolution	54
5.6	Mean displacements of $I$ , $I_g$ and $I_c$ for 20 image pairs at 4mm resolution	54
5.7	Mean displacements of $I$ , $I_g$ and $I_c$ for 20 image pairs at 2mm resolution	55



# Chapter 1

## Introduction

### 1.1 Background

Medical images have played an important role in clinical medicine and they can be divided into two basic categories: anatomical and functional images. Anatomical images include magnetic resonance imaging (MRI), computed tomography (CT) and ultrasound, etc. and functional images include positron emission tomography (PET), single photon emission computed tomography (SPECT) and functional MRI (fMRI), etc.

It is helpful in clinical medicine to use images of the same subject by different imaging modalities, since different imaging modalities are based on different physical principles and the captured images usually contain complementary information, e.g., to use anatomical and functional images for the purpose of tumor localization and follow up analysis. However, images from different modalities are often captured at separate scan sessions and in different views. It is therefore impossible to interpret the images

and integrate the information contained in them without beforehand transformation or registration, which brings the involved images into spatial correspondence and is discussed in the following section.

## 1.2 Concept of Image Registration

Image registration or matching brings two images of the same object captured at different time or from different imaging modalities into spatial correspondence. The spatial correspondence is described by a geometrical transformation that defines a spatial mapping of corresponding points in the two images. There exist several types of geometrical transformations that reflect the inherent spatial relationship between corresponding points of images. A rigid body transformation preserves the distance between points, and can be represented by two orthogonal translations and two orthogonal rotations for an image pair. A global scaling transformation is a rigid body transformation plus scale factors along two axes. An affine transformation maps parallel lines to parallel lines, but does not conserve the angles between lines and it consists of rigid body transformation plus scaling and shearing. A projective transformation maps straight lines to straight lines, but parallelism of lines is not preserved. The most general type is curved transformation that maps a line into a curve and therefore does not preserve the straightness of lines.

Another issue in image registration is interpolation, which will arise whenever non-integer spatial coordinates are produced in the process of geometrical transformation.



The simplest interpolation method is the nearest neighbor interpolation, which assigns the non-integer pixel the intensity of its nearest neighbor that has integer coordinates. Though its simplicity, the nearest neighbor interpolation method is not good enough to guarantee sub-pixel registration accuracy, as it is not sensitive to translations up to 1 pixel. More complicated and computation expensive interpolation methods exist [46], such as linear interpolation, cubic interpolation, trilinear partial volume distribution interpolation (PV) [6].

Multi-modal medical image registration is a special case of the general image registration problem, where the images need to register are captured from different medical image modalities and usually in different scanning sessions. Multi-modal medical image registration is more difficult than intra-modal image registration, because different modalities have different imaging principles, and hence the acquired images usually have different resolutions and intensity levels. The relationship between the intensities of such images is hence nonlinear. This observation has two indications. First, multi-modal image registration is a challenging problem. Second, registration methods that work well for intra-modal images are usually not suited for multi-modal images. A pair of multi-modal images is given in Fig. 1.1. Note the big visual difference of the two images. Even manual registration may not give satisfactory solution for these images.

Though the difficulty of registering multi-modal medical images, correctly registering them is very important in clinical medicine to integrate different information in the images for the purpose of diagnose and follow up analysis. In the specific example of

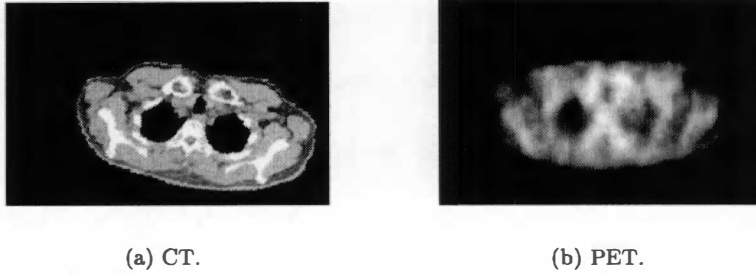


Figure 1.1: A pair of multi-modal medical images.

functional and anatomical images, functional images give indication of functional activation of human body and anatomical images delineate well anatomical structures, so they contain complementary information about the imaged target. Correctly combining these two kinds of information can indicate functional abnormality of specific anatomical locations and is then helpful for diagnosis, surgical planning and so on.

### 1.3 State of the Art

Over the years, a lot of methods have been proposed for multi-modal medical image registration. In early days, researchers registered medical images using fiducial marker-based methods [28], surface-fitting methods [30], correlation-based methods [47] or interactive methods [32], to name a few. Later, automatic and intensity-based methods have gained more research interest and become more popular. The merit of intensity-based methods lies in that they directly work on the intensity space of involved images and hence there is no need for feature extraction in these methods. More important

is that those methods can be used retrospectively and are therefore suited for clinical applications. Several survey papers are available in literature [28][48][50].

Mutual information is one of the measures utilizing intensity information and was proposed by two independent research groups in 1996 [15] and 1997 [25], respectively. Since it was proposed, mutual information has been intensively researched and shown general success in registering multi-modal medical images [44][36]. Besides the common advantages of intensity-based methods, mutual information-based method has several specific ones. The most important one might be that it can be used in diverse registration problems, e.g., intra-modal [14], inter-modal[15][25] and inter-individual[23] registrations. The only assumption it makes is that the two images need to register are statistically dependent. Besides, mutual information-based registration can be achieved fully automatically. Though the general success achieved by intensity-based mutual information, it is not a panacea. Proof has been gained to show mutual information may fail in some cases [12][40]. A possible reason is it does not consider the spatial information in the images at all. By working only on intensity space, mutual information-based methods got the merit of simplicity and automation and at the same time, it discards the important spatial information that exists in the images. This may lead to mis-registration in some cases.

Recently several groups proposed the integrating use of intensity and spatial information. Pluim *et al.* proposed to combine spatial and intensity information into one measure, which is the standard mutual information weighed by a term from the gradient

information of images [34]. Lundqvist *et al.* proposed another combination scheme to register inter-individual images, which combine the intensity-based mutual information and the mutual information based on gradients of the images [23].

## 1.4 Thesis Goal and Outline

In this thesis, we continue the work of combining intensity and spatial information and propose a combined mutual information measure to register multi-modal medical images. We define mutual information of the intensity and gradient of images. We show the proposed measure is actually a generalization of the intensity mutual information and gradient mutual information. This generalized mutual information utilizes both the intensity and spatial information in the images and integrates them into one measure. Maximizing this measure is assumed to correctly register the images. Powell's direction set method is used to optimize the rigid body transformation parameters. We first register slice images scanned in a single patient in the same or different scanning sessions. Then 20 pairs of co-registered CT and PET slice images at three different resolutions are used to study the performance of this measure and compare it to the intensity mutual information, gradient mutual information and two other combining measures. Experiment results indicate that the proposed combined measure produces reliable registrations and it outperforms the intensity- and gradient-based measures at all three resolutions.

The rest of thesis is organized as following. In chapter 2, a review of medical image

registration methods is given. In chapter 3, mutual information of an image is introduced with its limitation discussed. The combined mutual information of intensity and gradient is then proposed to improve the intensity mutual information. In chapter 4, optimization methods are briefly reviewed and Powell's conjugate direction set method is explained in detail. The registration results by optimizing the combined mutual information using Powell's method is presented in chapter 5. Chapter 6 summarizes this thesis with future work recommended.

## Chapter 2

# Literature Review

### 2.1 Overview

Multi-modal medical image registration has become an important branch of medical imaging. This development has two causes. First, the fast advance in computing technology has made it possible to register two volume images. This has made it feasible for registration methods that are based on the full contents of the images rather than on just a few points of artificial markers or anatomical landmarks. Second, there is a growing demand from the clinic for integrating information from multi-modal medical images, particularly in diagnosis, treatment planning and follow-up analysis.

This chapter reviews the literature on medical image registration and the focus is on methods that register medical images captured from multiple modalities. This excludes registration of images from the same modality and registration of images to atlas. Matching of series images are also not in the scope of this chapter.

## 2.2 Registration Methods for Multi-modal Medical Images

In [48], Van den Elsen *et al.* give a classification of medical image registration methods based on nine basic criteria. The main criteria include: nature of matching basis (extrinsic/intrinsic), dimensionality ( $2D/3D/4D$ ), elasticity of transformation (rigid-body/affine/projective/curved), interaction (automatic/semi-automatic/interactive), modalities involved (intra-modality/multi-modality/ modality-to-model/patient-to-modality). This section discusses rigid registration methods for multi-modal medical images.

We use the criterion of nature of matching basis to divide the methods into two groups: extrinsic and intrinsic approaches. Extrinsic methods utilize external artificial markers or objects that is intentionally attached to the subject during image acquisition stage, while intrinsic methods only use image information from the imaged subjects. In the next we will review registration methods based on this categorization.

### 2.2.1 Extrinsic Methods

There exist two major approaches under this group. A common property of these methods is that they can not be used in retrospective registration. This property requires the imaging protocols to include extra processing when acquiring images. Images acquired from multiple modalities without such pre-processing therefore can not be registered using these extrinsic methods.

### **Invasive Techniques**

In invasive methods, a stereo-tactic frame is rigidly screwed to the imaged subject and in the image acquisition stage, localizer frames containing point markers or line markers are attached to the stereo-tactic frame in order to provide a reference system for all imaging modalities[24][20]. This special procedure guarantees the accurate registration of all multi-modal images. The main drawback of the stereo-tactic frame-based registration lies in its prospective character. To apply this method, provisions must be made in the pre-acquisition stage and applying it is rather labor intensive. Besides, because of the invasive property of this kind of methods, they are the least patient friendly among all image registration approaches. Although stereo-tactic frame-based registration has been the most accurate registration method for a long time, intrinsic methods are reported to achieve similar or even high accuracy recently, while they are also more attractive in the point of view of other criteria.

### **Non-invasive Techniques**

Instead of using invasive stereo-tactic frame, non-invasive marking devices are used in these methods, such as mold, dental adapter and skin markers [19][41][11][9][51][52]. These methods are slightly less accurate than the stereo-tactic frame, but they are more patient friendly and can be used in more applications. Among all the extrinsic methods, skin marker-based method is the most patient friendly and is applicable to all clinical imaging modalities. The reproducibility of it is not good for long time intervals because



of the unintentional movement of subjects, however. Skin marker-based methods are not so labor intensive as the other extrinsic methods.

### **2.2.2 Intrinsic Methods**

The intrinsic registration methods have two properties in common. First of all, these methods can be used retrospectively; the imaging protocols hence do not need make extra provisions in the acquisition phase. The second is the extreme patient friendliness of these methods comparing to extrinsic methods. All that these methods need is the information contained in the images. However, how to use the image information is a problem. In other words, we have to choose image features on that the registration is based. In case of multi-modal medical image registration, it is not easy to select common features from quite dissimilar images.

Based on the features used in the matching procedure, intrinsic methods can be classified as point based, surface based or voxel based.

#### **Point-based**

Point-based methods rely on manually selected anatomical landmarks or automatically detected salient points appeared in both images [29][10]. These methods are rather labor intensive if the control points have to be selected interactively and their accuracy relies on the accurate localization of a sufficient number of control points in all modalities. In the case of multi-modal medical images, it is usually difficult to accurately select control points in both modalities involved, especially for functional images. As a result,

the reproducibility of this approach is low. The accuracy of this method will increase with the number of control points used until a certain limit is reached. Point-based techniques are applicable for a wide range of medical images and can be extended to elastic registration.

### **Surface-based**

Surface-based registration methods were initiated by Pelizzari *et al.* [21][30]. Contours from slices of one volume image are extracted and stacked together to form a three-dimensional surface and is called “head”. The same operation is performed on the other volume image and a subset of points of the surface form another three-dimensional model, called “hat”. Next mean distance from the points to the surface is iteratively minimized and the “hat” is then fitted onto the “head”.

Improvements on the original method have been reported from several groups, e.g., increasing the registration accuracy by removing outliers [17] and using automatic segmentation to eliminate human interaction during object matching [49].

Although surface-based methods are quite accurate, their robustness is questionable. Surface segmentation algorithms are generally highly data and application dependent and difficult to automate. For functional images it is not easy to find good contours and the surfaces are therefore hard to identify. Another problem of this method is the mis-match because of the anatomy symmetry property. If the anatomies registering are symmetric, there may be several perfect matches between the “head” and “hat”.

## Voxel-based

Registration methods based on voxel properties have been investigated from early 1990s. Since they are proposed, they have taken the lead in multi-modal medical image registration. These methods optimize a functional measuring the similarity of all geometrically corresponding voxel pairs for some features. Their main advantage is there is no need for feature extraction if only intensities are used, such that accuracy is not limited by segmentation errors as in point or surface based methods. As a consequence, most voxel-based methods do not require user interaction and thus are both labor extensive and reproducible. Other advantages of these methods consists of being retrospective, patient friendly and generally applicable to most image modalities. In addition, these methods can be extended to curved registration, which is a desired property in inter-subject registration.

In the methods of Woods *et al.* [54] and Hill *et al.* [13], they utilized the dispersion of the 2-D joint histogram to measure mis-registration. The 2-D joint histogram is constructed by counting the occurrence of corresponding voxel pairs in the overlapped area of two images and is assumed to be minimized when two images are registered. Collignon *et al.* [7][6] were inspired by the work of Hill and Woods to connect image registration with information theory and proposed to use entropy of the joint PDF of an image pair as a new registration measure. However, this measure is sensitive to partial overlap of the images, as it does not consider the information content of each of the images that will change during registration. As a consequence, when the homogeneous

background of two images coincide, the entropy will be minimized that will lead to wrong registration.

### MI-based Registration

Though mutual information-based method also belongs to voxel-based registration methods, it is worthy of treating it in a separate section because of its importance. Mutual information was proposed by two independent groups, Viola and Wells *et al.* at Massachusetts Institute of Technology and Collignon and Maes *et al.* at Katholieke University Leuven, Belgium, in 1996 [15] and 1997 [25], respectively. Mutual information is a basic concept from information theory and it measures the statistical dependence between two random variables or the amount of information that one variable contains about the other. Since it was proposed, mutual information has been intensively researched and shown general success in registering multi-modal medical images [44][36]. Besides the common advantages of intensity-based methods, mutual information based methods have several specific ones. The most important one might be that it can be used in diverse registration problems, e.g., intra-modal [14], inter-modal [15][25] and inter-individual [23] registrations. The only assumption it makes is that the two images need to register are statistically dependent. Besides, mutual information-based registration can be achieved fully automatically. Though the general success achieved by intensity-based mutual information, it may fail in some cases [12][40]. A possible reason is it does not consider the spatial information in the images at all. By working only on intensity space, mutual information-based methods got the merit of simplicity and

automation and at the same time, it discards the important spatial information that exists in the images. This may leads to mis-registration in some cases.

Spatial information in images is useful for registration. Measures based on spatial information have been proposed and successfully used in medical image registration [31][26][27] and intra-modal image registration [22]. Recently, several authors investigated image registration using mutual information defined on feature space [38][3][4]. In [38], Rangarajan *et al.* applied mutual information on extracted feature points. Butz and Thiran [3][4] used mutual information based on edgeness to register images. This method uses mutual information of image features instead of intensity and actually combines two types of registration methods. However, a pitfall of this kind of methods is that they discard a lot of information from the intensity images. It is then natural to think of integrating the intensity and spatial information. Pluim *et al.* [34] proposed to combine spatial and intensity information into one measure, which is the standard mutual information weighing by a term from the gradient information of images. Lundqvist *et al.* [23] proposed another combination scheme to register inter-individual images, which combine the standard intensity-based mutual information and the mutual information based on gradients of the images.

## 2.3 Summary

Research of multi-modal medical image registration has made huge progress in the last few years. Extrinsic methods are getting less popular because of their major drawbacks,

especially the prospective property and least patient friendliness. Intrinsic methods, in the other hand, can be used in retrospective registration and are very patient friendly and, as a consequence, are more popular than extrinsic methods. Among all the intrinsic methods, mutual information has gained intensive research and become the most popular method for multi-modal medical image registration. Besides the common advantages belonging to intrinsic methods, mutual information has its unique merits, e.g., mutual information can achieve high registration accuracy that is even comparable to that by extrinsic methods.

## Chapter 3

# Image Registration by Mutual Information

### 3.1 Definitions

Mutual information measures statistical similarity of two stochastic signals. The mutual information between the intensities of two images  $X$  and  $Y$  is defined by the use of entropies of the two images:

$$\tilde{I}(X, Y) = H(X) + H(Y) - H(X, Y) \quad (3.1)$$

where  $H(X)$  and  $H(Y)$  are the entropies, and  $H(X, Y)$  denotes the joint entropy of images  $X$  and  $Y$ . Popular Shannon entropy [36] of an image  $X$  is computed from the probability distribution of its intensities and is defined as

$$H(X) = - \sum_{a=0}^{N-1} P_A(a) \log P_A(a) \quad (3.2)$$

where  $P_A$  denotes the marginal probability density function (PDF) of the image intensities and  $N$  indicates the total number of bins used to compute the histogram. A marginal PDF can be estimated by normalizing the intensity histogram of the image. The entropy is actually a measure of information, or uncertainty associated with the event. If  $P_A$  is a uniform distribution, the entropy will be maximized, while the entropy of a deterministic signal will be minimized. The more a PDF is dispersed, the higher the entropy becomes. A joint entropy of two images  $X$  and  $Y$  can be computed from the joint probability distribution

$$H(X, Y) = - \sum_{a=0}^{N-1} \sum_{b=0}^{M-1} P_{A,B}(a, b) \log P_{A,B}(a, b) \quad (3.3)$$

where  $P_{A,B}$  is the joint PDF and can be directly estimated from the joint histogram of intensities of image  $X$  and  $Y$ . Similar with the entropy of an image, the joint entropy of two images measures the dispersion of the joint PDF. The more dispersed the joint PDF, the higher value the corresponding joint entropy.

Normalized mutual information was shown to produce similarly accurate results with mutual information and might have the advantage of insensitivity to the amount of overlapped area between two images. It can be defined as in the following equation [43]:



$$I(X, Y) = \frac{H(X) + H(Y)}{H(X, Y)} \quad (3.4)$$

where  $H(X)$  and  $H(Y)$  are the entropies of images  $X$  and  $Y$  and  $H(X, Y)$  is the joint entropy of them. Their definitions are given in Eq. 3.2 and Eq. 3.3, respectively. Some basic properties of normalized mutual information can be derived [8][1].

$$\textit{Symmetry} : \quad I(X, Y) = I(Y, X) \quad (3.5)$$

$$\textit{Boundness} : \quad 1 \leq I(X, Y) \leq 2 \quad (3.6)$$

$$\textit{Self Information} : \quad I(X, X) = 2 \quad (3.7)$$

Another definition for normalized mutual information, Entropy Correlation Coefficient (ECC), is presented in [25].

$$ECC(X, Y) = \frac{2\tilde{I}(X, Y)}{H(X) + H(Y)} \quad (3.8)$$

where  $\tilde{I}(X, Y)$  is the mutual information of images  $X$  and  $Y$  and  $H(X)$  and  $H(Y)$  are entropies of the overlapped area of the two images. The two normalized versions are actually related by one-to-one mapping and the relation is:

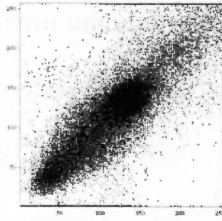
$$ECC(X, Y) = 2(1 - \frac{1}{I(X, Y)}) \quad (3.9)$$

From now on in the thesis, we use mutual information to represent the normalized version defined in Eq. 3.4 if there is no other note.

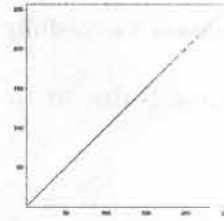
### 3.2 Mutual Information of Intensity

When two images are correctly registered, the corresponding joint PDF of intensities is compact and the corresponding joint entropy will hence be small. If the images are misaligned, the joint PDF is dispersed and the joint entropy will be relatively high. The joint PDFs of a pair of identical CT images before and after registration in Fig. 3.1 illustrate this characteristic. In that figure, the joint entropy gets smaller when the image pair is in registration. Based on this direct relationship between the dispersion of PDF and the goodness of registration of images, the registration of an image pair is achieved by minimizing the joint entropy between them [7][42]. However, joint entropy is sensitive to partial overlap of the images, as it does not consider the information content of each of the images that will change during registration. As a consequence, when the homogeneous background of two images coincide, the entropy will be minimized that will lead to wrong registration [12].

Mutual information of intensity considers both the joint entropy and the entropies of the intensities of two images and is less sensitive to the overlapped area between the two images. Fig. 3.2 illustrates that the intensity mutual information finds the amount of mis-alignment of the two images to be registered. The two synthetic images have different brightness intensities and one of them is shifted along the horizontal axis by

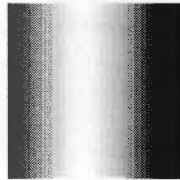


(a) Joint entropy: 2.05

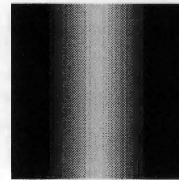


(b) Joint entropy: 1.35

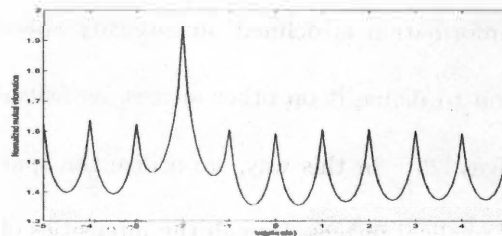
Figure 3.1: Joint PDF and corresponding joint entropy values of an image pair before and after the registration. (a) Mis-registration, (b) Perfect registration



(a) Image A



(b) Image B



(c) Intensity mutual information

Figure 3.2: A synthetic example where the intensity mutual information successfully registers the images. (a) A  $30 \times 30$  strip image, (b) is gotten by subtracting 5 to every pixel of (a) and shifting 2 pixels horizontally. (c) The intensity mutual information when (b) is registered to (a).

two pixels. Though the image pair involved has different intensity levels, the intensity mutual information successfully registers them. The local minimum prominent in the registration curve is due to the interpolation [46]. The peak correctly indicates the translation.

While the intensity mutual information gained promising successes, it may fail in some cases [12][40]. A possible reason for this is it only considers the intensity information in two images, not the spatial information. Fig. 3.3 gives another synthetic registration problem where the intensity mutual information fails to correctly register the images. It is interesting and important to note that, after randomizing the intensity of each strip in the input image B, the registration function of mutual information remains unchanged comparing to the un-randomized case.

### 3.3 Mutual Information of Gradient

The intensity mutual information is defined on intensity space; it is a natural and straightforward extension to define it on other spaces, as feature point [38], edgeness [3] and gradient of images [23]. In this way, we utilize the spatial information in the images. In multi-modal medical images, though the intensities of images from different modalities are different, edges exist between transitions of tissues, which correspond to strong gradient magnitudes. If the involved modalities image the same anatomical structure, we can expect corresponding gradients.

Edges can be computed by convolving an image with local kernels such as a Sobel

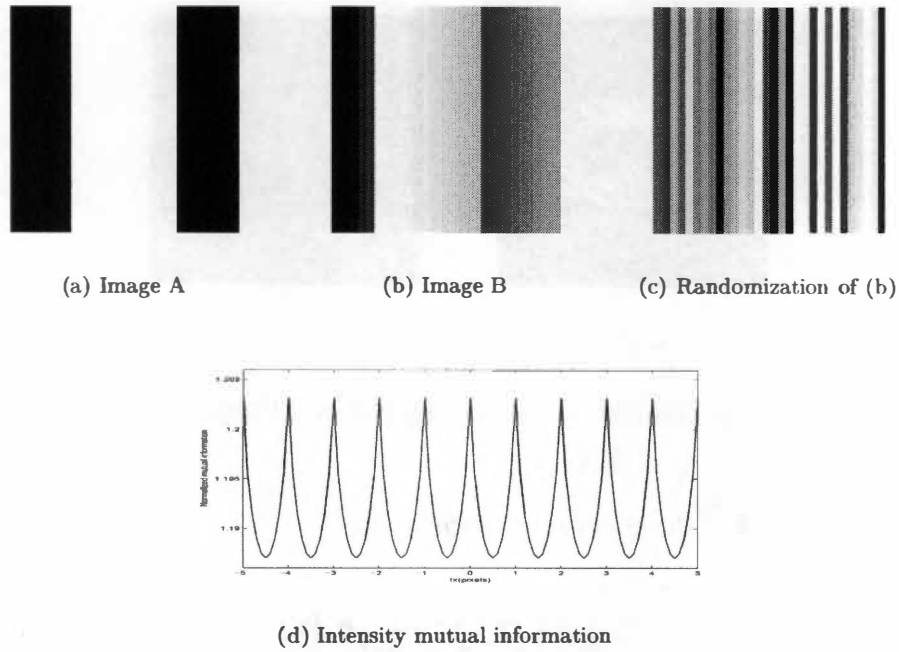


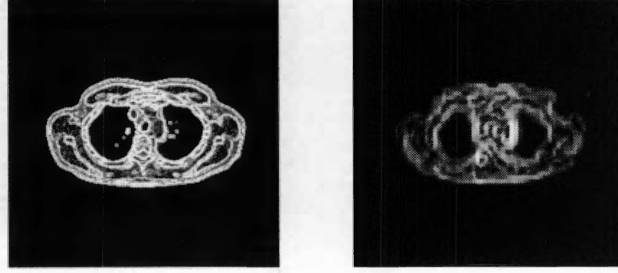
Figure 3.3: Illustration of the limitation of the intensity mutual information. (a) The base image A, (b) The input image B, (c) A randomized version of the input image, (d) The intensity mutual information when (b) or (c) is registered to (a). (Adapted from Roche *et al.* [40])

operator. Sobel kernels detect horizontal and vertical intensity contrast. Set the two components of gradient  $\mathbf{g}$  of an image voxel are  $g_x$  and  $g_y$ , the magnitude of the gradient is then calculated by:

$$|\mathbf{g}| = \sqrt{g_x^2 + g_y^2} \quad (3.10)$$

Fig. 3.4 shows examples of the edges of a pair of CT and PET images by use of the Sobel kernels.

After get the gradient magnitudes of two images, we can define the normalized



(a) PET

(b) CT

Figure 3.4: Gradient magnitude of a pair of CT and PET images

mutual information of the gradient as the following.

$$I_g(X, Y) = \frac{H_g(X) + H_g(Y)}{H_g(X, Y)} \quad (3.11)$$

Where  $H_g(X)$  and  $H_g(Y)$  are entropies of the gradient magnitudes of image  $X$  and  $Y$ , respectively and  $H_g(X, Y)$  is the joint entropy of them. They are computed by the following equations:

$$H_g(X) = - \sum_{c=0}^{N-1} P_C(c) \log P_C(c) \quad (3.12)$$

$$H_g(X, Y) = - \sum_{c=0}^{N-1} \sum_{d=0}^{M-1} P_{C,D}(c, d) \log P_{C,D}(c, d) \quad (3.13)$$

Where  $P_C$  and  $P_{C,D}$  denote the marginal and joint PDF of the gradient magnitudes of the images. The subscript  $g$  in the above equation is to indicate that all terms are

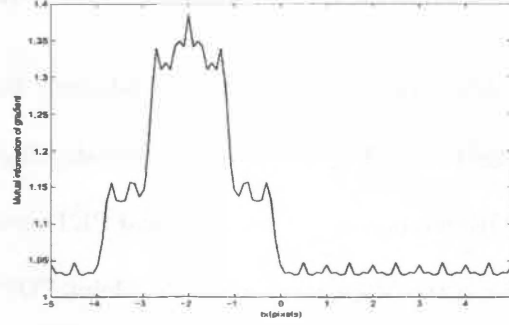


Figure 3.5: Registration function of the two images in Fig. 3.3

defined for the gradient of images.

In Fig. 3.3 we have shown a synthetic registration problem where the intensity mutual information fails to correctly register the images. By applying the gradient mutual information to the same images in Fig. 3.3 (a) and (b), we get the registration function of horizontal translations that is shown in Fig. 3.5. In this figure, the maximum of the gradient mutual information correctly indicates the true translation between the two images.

By defining the mutual information of the gradients, we use the spatial information in images. However, a lot of intensity information in the two images is discarded by doing also. In the next heading, we will introduce the proposed measure, which use both the intensity and gradient information of two images.

### 3.4 Combined Mutual Information for Image Registration

This thesis proposes combined mutual information of intensity and gradient for multi-modal medical image registration. Fig. 3.6 shows a schematic diagram of the proposed registration procedure. Given a pair of CT image  $X$  and PET image  $Y$  to register,  $Y$  is first transformed to  $Y'$  by a transformation matrix  $T$ . Joint PDF  $P_{ABCD}$  is estimated from the intensity and gradient magnitudes of  $X$  and  $Y'$  in the overlapped area of them and the combined mutual information  $I_c$  is then calculated from this joint PDF. Finally, Powell's optimization method is used to search the optimal transformation matrix  $T_m$  that corresponds to the maximum of the combined mutual information.

Intensity and gradient provide useful information in registration. The mutual information in gradient space integrates the spatial information into the mutual information measure. But if we only use the gradient information to register multi-modal medical images, a lot of information in the intensities is discarded and hence the registration may not be robust, especially when the images are in low resolution or strong noise presents.

The standard mutual information is extended to include the spatial information besides the intensity information. For each pair of voxels, intensities and gradient magnitudes are used to construct a joint histogram. Then the combined normalized mutual information is defined as in the following equation:

$$I_c = \frac{H_i(X) + H_g(X) + H_i(Y) + H_g(Y)}{H_{i,g}(X, Y)} \quad (3.14)$$



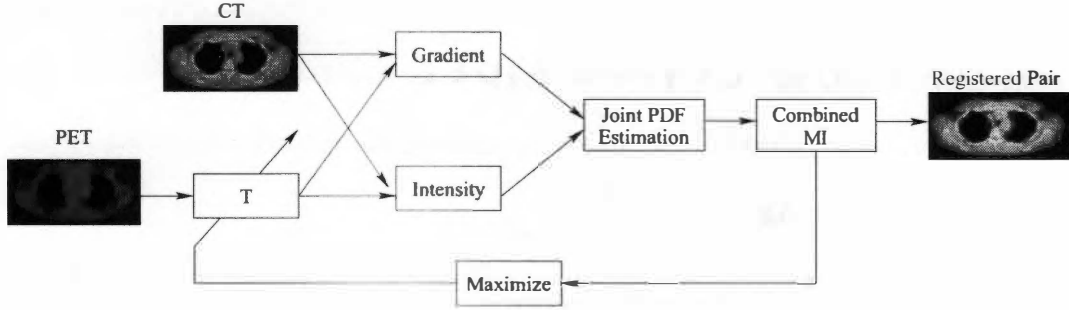


Figure 3.6: CT-PET image registration by the proposed combined mutual information.

where  $H_{i,g}(X, Y)$  is the joint entropy of image intensities and gradients and is defined in Eq. 3.15.

$$H_{i,g}(X, Y) = - \sum_{a=0}^{N_1-1} \sum_{b=0}^{N_2-1} \sum_{c=0}^{N_3-1} \sum_{d=0}^{N_4-1} P_{A,B,C,D}(a, b, c, d) \log P_{A,B,C,D}(a, b, c, d) \quad (3.15)$$

where the joint PDF  $P_{A,B,C,D}$  is estimated from the joint histogram of the intensities and gradient magnitudes of image  $X$  and  $Y$ .  $N_1$ ,  $N_2$ ,  $N_3$  and  $N_4$  are the bin sizes used to compute the joint histogram along each axes.  $H_i(X)$ ,  $H_i(Y)$ ,  $H_g(X)$  and  $H_g(Y)$  are the entropies of the intensities and gradient magnitudes of image  $X$  and  $Y$ , respectively.

Phase angle between gradients are not used in the combined measure because in multi-modal images, the same tissue may have different intensities as a result of the different characteristic of imaging modalities. Hence the gradients of the images may point in diverse directions. So only magnitudes of the gradients are used in the computation of generalized normalized mutual information. All magnitudes are linearly scaled properly before they are used to compute the joint histogram.

While the intensity mutual information emphasizes the volumetric information and risks to neglect the important spatial information, we emphasize both volumetric and spatial information existed in the images by defining the mutual information on the combined intensity and gradient space.

In analogy with the joint histogram on intensities of two images, where mis-registration of the two images corresponds to dispersion in the histogram and a compact histogram means the two images are in good registration, here we define the joint histogram based on both the intensities and gradient magnitudes. It plots intensities and gradient magnitudes of corresponding voxels in the overlapped area of two images in a hyper-plane. If two images are correctly registered, we expect hyper-clustering in the joint histogram to appear and the corresponding mutual information value should be high. Maximizing the mutual information on the combined space is then assumed to correspond to the correct registration.

The generalized measure defines the mutual information on the combined intensity and gradient probability distribution. To relate it to the standard intensity mutual information, we only need to note that the intensity probability distribution can be obtained by summing over the two gradient magnitude axes of the combined probability distribution. This is similar with the relationship between the 2-D joint probability distribution and its marginal probability distributions.

[*Theorem*] The combined mutual information  $I_c$  is the generalization of the individual intensity and gradient mutual information  $I$  and  $I_g$  and can be equal to them in the

extreme situations.

*Proof:* First assume the intensity PDF and gradient magnitude PDF is independent, i.e.,

$$P_{A,B,C,D}(a, b, c, d) = P_{A,B}(a, b) \cdot P_{C,D}(c, d) \quad (3.16)$$

Then we have

$$\begin{aligned} H_{i,g}(X, Y) &= \sum_a \sum_b \sum_c \sum_d P_{A,B,C,D}(a, b, c, d) \log P_{A,B,C,D}(a, b, c, d) \\ &= \sum_a \sum_b \sum_c \sum_d P_{A,B}(a, b) \cdot P_{C,D}(c, d) \log P_{A,B}(a, b) \cdot P_{C,D}(c, d) \\ &= \sum_a \sum_b P_{A,B}(a, b) \log P_{A,B}(a, b) \left( \sum_c \sum_d P_{C,D}(c, d) \right) + \\ &\quad \sum_a \sum_b P_{A,B}(a, b) \left( \sum_c \sum_d P_{C,D}(c, d) \log P_{C,D}(c, d) \right) \\ &= \sum_a \sum_b P_{A,B}(a, b) \log P_{A,B}(a, b) + \\ &\quad \sum_a \sum_b P_{A,B}(a, b) \left( \sum_c \sum_d P_{C,D}(c, d) \log P_{C,D}(c, d) \right) \end{aligned} \quad (3.17)$$

If we further assume the gradient magnitudes of images are constant, i.e., the PDF of the gradient magnitudes has only one peak, then the second term in the above equation will vanish, and we then get

$$\begin{aligned} H_{i,g}(X, Y) &= \sum_a \sum_b P_{A,B}(a, b) \log P_{A,B}(a, b) \\ &= H(X, Y) \end{aligned} \quad (3.18)$$

and

$$H_g(X) = 0 \quad (3.19)$$

$$H_g(Y) = 0 \quad (3.20)$$

Input Eq. 3.18, Eq. 3.19 and Eq. 3.20 into Eq. 3.14 and compare it to the definition of intensity mutual information in Eq. 3.4, we get  $I_c \equiv I$ . Similarly, it can be shown that  $I_c \equiv I_g$  with certain conditions satisfied.

Since the combined measure could be equal to the individual intensity or gradient mutual information measures in the extreme situations, the conclusion, that the intensity mutual information and the gradient mutual information is a special case of the generalized mutual information measure, might therefore be safely drawn. The combined measure is hence the generalization of the intensity and gradient mutual information.

### 3.5 Transformation Model

The rigid-body transformation model [53] concerns the relationship between the coordinates of the two images under spatial transformations. Displacement and rotation angle are the parameters associated with the rigid-body transformation. Given a pair of vectors of corresponding voxels  $\mathbf{p}'$  and  $\mathbf{p}$  in the transformed and original images, respectively, they are related by the transformation matrix  $T$  by the following equation:

$$\mathbf{p}' = T\mathbf{p} \quad (3.21)$$

where  $\mathbf{p}' = [\mathbf{x}' \quad \mathbf{y}' \quad 1]^t$  and  $\mathbf{p} = [\mathbf{x} \quad \mathbf{y} \quad 1]^t$ . If rigid-body transformation model is used,  $T$  is equal to:

$$T = \begin{bmatrix} \cos \theta & -\sin \theta & \Delta x \\ \sin \theta & \cos \theta & \Delta y \\ 0 & 0 & 1 \end{bmatrix} \quad (3.22)$$

where translation is represented by the parameters  $\Delta x$  and  $\Delta y$ . The parameter  $\theta$  indicates the rotation angle. In the experiment presented in the next section, rigid-body transformation model is assumed between the base and input images. Registration is achieved by optimizing three parameters, i.e., rotation and two translations.

### 3.6 Mutual Information Weighed by Gradient Term

Pluim *et al.* [34] add a gradient-based weighing term to the intensity mutual information to form the new combined measure, which, we name as  $I_p$  for the sake of convenience, is defined as:

$$I_p(X, Y) = C(X, Y)I(X, Y) \quad (3.23)$$

where  $I(X, Y)$  is the standard intensity-based normalized mutual information as defined in Eq. 3.4 and  $C(X, Y)$  is a weighing term based on the gradient information of images, which is defined as

$$C(X, Y) = \sum_{(\mathbf{p}, \mathbf{p}') \in (\mathbf{X} \cap \mathbf{Y})} w(\alpha_{\mathbf{p}, \mathbf{p}'}(\sigma)) \min(|\nabla \mathbf{p}(\sigma)|, |\nabla \mathbf{p}'(\sigma)|) \quad (3.24)$$

where  $\mathbf{p}$  and  $\mathbf{p}'$  are corresponding voxels in the overlapped area of the base and input image, respectively and  $\alpha$  is the angle between the corresponding gradient vectors  $\nabla\mathbf{p}$  and  $\nabla\mathbf{p}'$  and is defined by:

$$\alpha_{\mathbf{p},\mathbf{p}'}(\sigma) = \cos^{-1} \frac{\nabla\mathbf{p}(\sigma) \cdot \nabla\mathbf{p}'(\sigma)}{|\nabla\mathbf{p}(\sigma)| |\nabla\mathbf{p}'(\sigma)|} \quad (3.25)$$

The authors use the weighing function defined in Eq. 3.26 to favor angles that are approximately equal to zero or  $\pi$ . The angle function is then multiplied by the minimum of the gradient magnitudes of corresponding voxels in both images to favor the case where gradients in both images are strong.

$$w(\alpha) = \frac{\cos(2\alpha) + 1}{2} \quad (3.26)$$

They calculated the components of gradient in each dimension by convolution of the images with the appropriate first derivative of a Gaussian kernel of scale  $\sigma$  and  $\sigma$  is chosen as 1.5 mm in their experiment based on their past research experience. In our implementation of  $I_p$ , we use the Sobel kernels to calculate the gradient. By doing so, we intended to extract the gradient information in a unified way for all the measures in the comparison study.

One can also think of integrating the two right terms in Eq. 3.23 by adding them together. But, as the authors mentioned, if addition is used, normalization of the two terms are required and hence more computation and complexity are induced.

### 3.7 Multiplication of Intensity- and Gradient-based Mutual Information

In [23] Lundqvist *et al.* propose another combining measure to register inter-individual images. In their measure, the intensity- and gradient-based normalized mutual information are computed separately and then the two terms are multiplied to form the new combined measure.

$$I_t(X, Y) = I(X, Y)(I'_g(X, Y) + R) \quad (3.27)$$

where  $R$  is a regularization term and is selected before the registration. Based on the experiment results presented by the authors and results from our experiment, we choose an intermediate value of 5 for the regularization term in the comparison study.

The gradient-based mutual information  $I'_g$  in Eq. 3.27 is slightly different with that in Eq. 3.11 by estimating the joint PDF from the gradient magnitudes plus phase angle. Phase angle is used as the third feature dimension in this measure to emphasize the homogeneous gradient direction in the inter-individual images. The components of gradients are approximated by convolution of the images with a simple kernel,  $[-1 \ 0 \ 1]$ , in each dimension. In our implementation of  $I_t$ , we use the Sobel kernels to calculate the gradient whenever it is needed, as afore mentioned.

## Chapter 4

# Optimization of Registration Measure

### 4.1 Problem Statement

Maximization of the registration measure is an optimization process that finds the optimal transformation for an image pair. Given a base image  $X$  and an input image  $Y$ , we want to find the transformation matrix  $T_m$  that will maximize the registration measure between the base image and the transformed input image by  $T_m$ , i.e.,

$$T_m = \arg \max_T (f(X, T(Y))) \quad (4.1)$$

Where  $f$  maybe one of the registration measures discussed in the previous chapter. The registration measure actually defines an  $n$ -dimensional function of the transforma-



tion, with  $n$  the degrees of freedom of the transformation. When rigid transformation is used,  $n$  is equal to three and the transformation matrix  $T$ , accordingly, includes three variables, i.e., rotation angle  $\theta$  and two translations  $\Delta x$  and  $\Delta y$ . The maximum of this function is assumed to correspond to the transformation that correctly registers the images. Maximization of the registration measure is therefore a multi-dimensional optimization problem.

The bad news is the registration function is usually not a smooth function, instead, it contains many local maxima. Some of the local maxima is resulted from a local good registration of the two images, while the others are related to implementation issues, e.g. intensity interpolation for non-integer voxels. Different interpolation methods have been investigated to reduce the local maxima in [46]. Because of the local maxima problem, the final registration results depend largely on the optimization method used. It is obvious that the optimization will lead to a mis-registration if it gets struck into a local maximum.

Another important issue related to the optimization is the capture range of the maximum. The desired maximum may be the “global” maximum of only part of the entire search space, while the true global maximum of the whole search space may not be the desired one. This has two consequences for optimization. First, the optimization is sensitive to the starting search position and an optimization started outside the capture range has little chance to find the desired maximum. Secondly, the global optimization methods such as simulated annealing and genetic algorithm, may not lead to correct

solution, if there are no adaptation made to them.

In the next section, we will briefly review the commonly used optimization methods for medical image registration. Powell's method, which is chosen to be implemented in this thesis, is then discussed in detail.

## 4.2 Overview of Optimization Methods

Optimization methods can be divided into two categories based on whether the method needs gradient information or not [36]. The methods that do not need to compute gradients include Powell's method, Simplex method and hill-climbing method, while methods in the other category include gradient ascent method and quasi-Newton method.

Powell's method is very popular for medical image registration. This method optimizes the registration function along a set of conjugate directions sequentially until a certain criterion is reached. The drawback of Powell's method, which is shared with all other local optimization methods, is the sensitivity to the local maxima existed in the registration function. Simplex method is another popular method in this field. Different to the Powell's method, Simplex method considers all the transformation variables simultaneously. Some modified methods of the standard Powell and Simplex methods are proposed to improve the performance. Plattard *et al.* [33] use a combination of the Powell and Simplex methods, while Kagadis *et al.* [18] combine Powell's method and the genetic algorithm. Jenkinson and Smith [16] propose an optimization technique that adds initialization and multi-start to Powell's method.

Another categorization for optimization methods is to divide them into either local or global methods. Although most of the methods in use are local optimization, there are global methods used in registration such as genetic algorithm and simulated annealing. Genetic algorithm [3] is one of the evolutionary algorithms and is inspired by computation in biological systems. This method has been popularly used in search, optimization and machine learning. The merit of this method is it can find global solution given enough evolution time, while the drawback of it is also very significant, i.e., the evolution is very time consuming and it usually takes a long time to find the global solution. Simulated annealing [39] is another global optimization method, which escapes local maxima by occasionally moving to a smaller function value.

### 4.3 Multi-dimensional Optimization

The strategy for multi-dimensional optimization is to search along a set of directions so that optimization along any one of these directions does not affect the optimization already achieved by previous searches. Such a set of directions is known as conjugate directions. Along each of the directions, 1-D optimization is performed to find the maximum along that direction.

### 4.3.1 Conjugate Directions

Set point  $\mathbf{P}$  is the origin of the coordinate system with coordinates  $\mathbf{x}$ . A  $N$ -dimensional function  $f$  can be approximated at this point by its Taylor series as:

$$f(\mathbf{x}) = f(\mathbf{P}) + \sum_{i=1}^N \frac{\partial f}{\partial x_i} x_i + \frac{1}{2} \sum_{i=1}^N \sum_{j=1}^M \frac{\partial^2 f}{\partial x_i \partial x_j} x_i x_j + \dots \quad (4.2)$$

$$f(\mathbf{x}) \approx c + \mathbf{b}^t \mathbf{x} + \frac{1}{2} \mathbf{x}^t \mathbf{A} \mathbf{x} \quad (4.3)$$

where  $c$  is the function value at point  $\mathbf{P}$ ,  $\mathbf{b}$  is the first partial derivative of the function at point  $\mathbf{P}$  and  $\mathbf{A}$  is the Hessian matrix of function  $f$  at point  $\mathbf{P}$ . The gradient of  $f$  can be calculated from Eq. 4.3 as:

$$\nabla f = \mathbf{A}^t \mathbf{x} + \mathbf{b} \quad (4.4)$$

Suppose that we have searched along direction  $\mathbf{u}$  and found a minimum. Next we need to search along a new direction  $\mathbf{v}$  and require this new search does not affect the optimization achieved in the previous search. For this end, the gradient has to stay perpendicular to  $\mathbf{u}$  when searching along direction  $\mathbf{v}$ , i.e., that the change in the gradient must be perpendicular to  $\mathbf{u}$  and the following equation therefore holds based on Eq. 4.4.

$$\mathbf{u} \cdot \delta(\nabla f) = \mathbf{u} \cdot (\mathbf{A}^t \delta(\mathbf{x})) = \mathbf{u} \cdot (\mathbf{A}^t \mathbf{v}) = 0 \quad (4.5)$$

When two vectors  $\mathbf{u}$  and  $\mathbf{v}$  satisfy Eq. 4.5, they are said to be conjugate. When

each pair of directions in a set satisfies this condition, they are mutually conjugate directions. If we do successive line minimization of a  $N$ -dimensional function with quadratic form along  $N$  conjugate directions, we can reach the minimum of this function. If the function is not in the quadratic form, repetition of  $N$  line minimization will quadratically converge to the minimum. So the key issue of the a multi-dimensional optimization method is to find a set of conjugate directions. Once these directions are found, the left issue is to search the maximum along these directions by 1-D optimization routines.

#### 4.3.2 Powell's Method

Powell's method [37] is a multi-dimensional optimization algorithm that can produce  $N$  mutually conjugate directions. For an  $N$ -dimensional optimization problem, this method can be described by the following algorithm.

1. Set the starting point  $\mathbf{P}_0$  and initialize the set of directions to the basis vectors

$$\mathbf{u}_j = \mathbf{e}_j, \quad j = 1, 2, \dots, N$$

2. For  $j = 1, 2, \dots, N$ , move the current minimum point  $\mathbf{P}_{j-1}$  to the next minimum point  $\mathbf{P}_j$  along each direction  $\mathbf{u}_j$
3. Save  $\mathbf{u}_j \rightarrow \mathbf{u}_{j-1}$ ,  $j = 1, 2, \dots, N$ ,
4. Save the new direction  $(\mathbf{P}_N - \mathbf{P}_0) \rightarrow \mathbf{u}_N$

5. Move  $\mathbf{P}_N$  to the minimum along direction  $\mathbf{u}_N$  and save it in  $\mathbf{P}_0$ .
6. Repeat step 2 until cost function stops decreasing

Powell showed that  $N$  iterations of the above basic procedure would produce  $N$  mutually conjugate directions. However, this original version is seldom used in practice because it may produce directions that are linearly dependent. To overcome this problem, several modifications are available. One modification is to discard the old direction along which the function achieves its largest decrease after each single iteration, while the original version of Powell's method always discards the first direction  $\mathbf{u}_1$  and adds a new direction  $\mathbf{P}_N - \mathbf{P}_0$ . We adopted in our implementation this modified version instead of the original one. Along each direction, Golden section search explained in the following section is performed to find the maximum along that direction.

#### 4.3.3 Golden Section Search

Golden section search is a simple 1-D optimization method and it does not need to compute the gradient of the target function. This method is implemented in the thesis as the 1-D search routine.

The basic idea of golden section method can be summarized as: given three initial points  $a$ ,  $b$  and  $c$ , the algorithm tests the next point  $x$  that is 0.38197 of the bigger one of the two segments away from the central point  $b$ . If we assume  $x$  lies between points  $b$  and  $c$ , then if  $f(b) > f(x)$ , then  $a, b, x$  is the next triplet, otherwise,  $b, x, c$  is the next triplet. In all cases, the middle point of the triplet is the point with maximum ordinate.

Repeat this procedure until the distance between the two outer points is within some tolerance.

Fig. 4.1 gives an example illustrating the above search procedure. In this figure, 1, 3 and 2 are the initial points and they bracket a maximum. The function is first evaluated at point 4, then point 2 is replaced by point 4 and the new triplet becomes 1, 3 and 4. Then evaluate the function at point 5 and 6 in order. The final triplet in this figure is 5, 3, 6 that brackets the maximum, however we can repeat this procedure and further approach the desired maximum.

The above algorithm assumes that the initial points are given and the maximum is really bracketed by them. When solving a practical problem, these initial points are usually not available by themselves and need to be estimated by us using some method. An obvious method is to guess the first point and then step uphill to find the second point. The third point is estimated by taking a large enough step to stop the uphill trend. After this procedure, the second point is between the two outer points and the

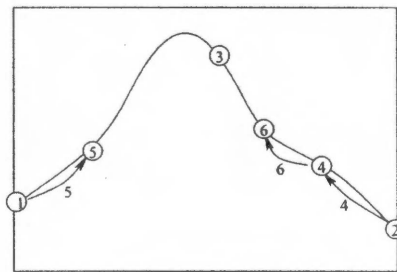


Figure 4.1: Golden section search for 1D optimization (Adapted from [37])

function at this point has the largest value. However, the step size should be carefully selected based on specific application. Too large or small a step size may make the search miss the desired maximum.



## Chapter 5

# Experiment Results

### 5.1 Dataset Description

In the experiments, we used three sets of CT and PET images. Images in each set were acquired on a single patient in the same or different scanning sessions with combined PET/CT scanner manufactured by CTI PET Systems (CPS, Knoxville, TN) [2]. The combined PET/CT scanner consists of a Siemens Emotion CT scanner mounted together with a CPS HR+ PET scanner, with a known axial offset between the two devices.

In the first dataset, CT and PET images are scanned in the same session and the CT and PET data are therefore intrinsically registered with a known axial offset. The offset is further rectified to make the CT and PET images are exactly registered and there is no transformation between them. The Detailed description is in Table 5.1.

To numerically compare the performance of the registration measures discussed in this thesis, two dimensional transaxial CT and PET slice images are extracted from

Table 5.1: Description of dataset one

Image Type	Voxel Size (mm)	Acquisition Date
CT	$(0.97 - 0.98)^2 \times 5$	06/20/2001
PET	$(5.14 - 5.15)^2 \times 2.425$	06/20/2001

the co-registered CT and PET volume images. Resolution adjustments are finished before the registration as the CT and PET have different voxel sizes and hence different resolutions. To study the performance of the measures under different resolutions, we interpolate the original slice image and acquire CT and PET images with resolutions of 8mm, 4mm, and 2mm. As PET images have resolution of about 5mm, they are up-sampled or down-sampled to get desired resolutions. While the original CT images have much higher resolution slightly less than 1mm, they are down-sampled to get coarser images. We use linear interpolation method in all the up- and down-sampling processing.

In the second dataset, the patient was scanned by the combined CT/PET scanner at two different days and two different tracers of PET were used in the two studies. The CT images from both studies are visually compared to extract CT slice images in one study and their corresponding PET slice images in the other study. Then the corresponding CT and PET slice images with unknown transformation are registered. The detailed description of the CT and PET images used is given in Table 5.2.

In the third dataset, the patient before and after a therapy was scanned by the same CT/PET scanner in two studies. In the same way of the second dataset, the CT slice

Table 5.2: Description of dataset two

Image Type	Voxel Size (mm)	Acquisition Date
CT	$(0.97 - 0.98)^2 \times 2$	12/19/2003
PET	$(4.06 - 4.07)^2 \times 2$	03/05/2004

Table 5.3: Description of dataset three

Image Type	Voxel Size (mm)	Acquisition Date
CT	$(0.97 - 0.98)^2 \times 5$	02/20/2002
PET	$(5.14 - 5.15)^2 \times 2.425$	09/10/2001

images from one study are registered to their corresponding PET slice images from the other study. The detailed description of the images used are given in Table 5.3.

All images are in DICOM format (Digital Imaging and Communications in Medicine), which is created to facilitate the storing and exchanging of medical images from different devices and is jointly developed by ACR (American College of Radiology) and NEMA (National Electrical Manufacturers Association). It sets up a uniform standard to transfer data definitions and information objects between different imaging systems; Equipment and applications can easily exchange information if they all conform to the standard. There are three versions of the standard so far and the latest version is DICOM 3.0 that is released in 1993. CT images are acquired in CT DICOM format and PET images are acquired in PET DICOM format.

## 5.2 Registration Error Estimation

An issue that so far has remained undiscussed is the evaluation of registration algorithms regarding to accuracy, while estimating the accuracy of a registration result is not an easy task, especially for CT-PET registration, because they are usually acquired in different scanning sessions and hence the true solution is not available. Usually the accuracy is evaluated qualitatively by visual inspection, and quantitatively by comparing the estimated transformation to that obtained by other registration techniques, such as extrinsic methods. In our experiment, visual inspection is performed to the registration results for the second and third datasets, since the gold transformation is unknown for these images. Example registration results for these two datasets are given in the following section. For images in the first dataset, because they are acquired in the same scanning session with the special combined scanner, CT and PET images are actually co-registered and there is fixed axial offset and no rotation between them. Axial offsets between CT and PET images were further rectified before the experiment is performed. Such data make it possible to quantitatively compare the accuracy of a registration result without employing other registration methods to get a gold solution. By using these data in our experiment, we are able to use a special technique to calculate the registration error of the proposed measure and further compare the performance of different measures.

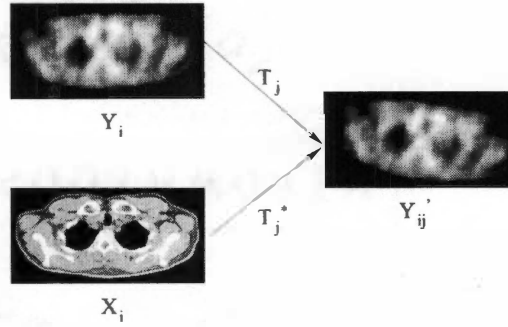
The main idea of our validation method is to apply known transformation, then estimate the transformation and finally compute the mean displacement of a set of voxels

of interest by applying the known and estimated transformation parameters to those voxels. The central square portion of the imaged subject at each resolution is chosen as the voxels of interest. It was done by first applying randomly generated parameters to the PET image of an image pair and then trying to estimate the parameters that register this transformed version of PET to its corresponding CT image and finally the mean displacement of a set of voxels of interest is computed.

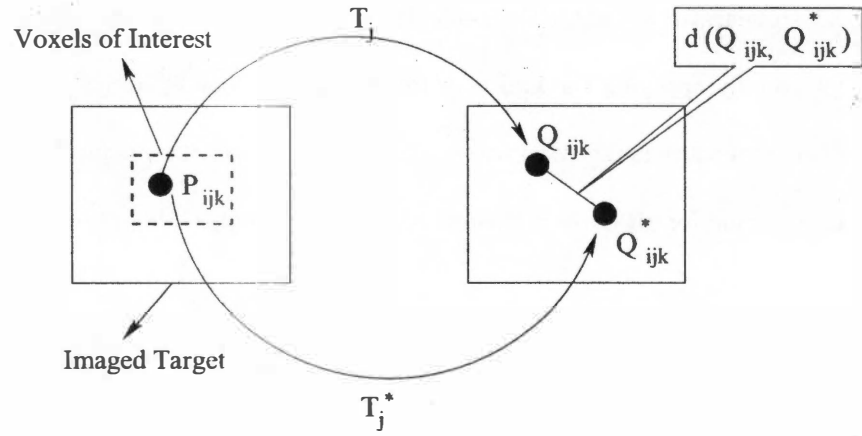
In Fig. 5.1, we illustrate the procedure for calculation of the mean displacements. Set a CT image as  $X_i$  and PET image  $Y_i$ . First transform  $Y_i$  using a randomly generated transformation matrix  $T_j$  and name the transformed PET image as  $Y'_{ij}$ . Then all the measures are used to register  $X_i$  to  $Y'_{ij}$  and the estimated transformation matrix is  $T_j^*$ . Registration error is then calculated as the Euclidean distance of a set of voxels of interest by applying the two transformation matrices  $T_j$  and  $T_j^*$  to those voxels. The basic procedure is repeated using different sets of parameters for 20 image pairs and the mean value for all pairs is then computed according to the following equation.

$$\bar{\epsilon} = \frac{1}{n_1} \frac{1}{n_2} \frac{1}{n_3} \sum_{i=1}^{n_1} \sum_{j=1}^{n_2} \sum_{k=1}^{n_3} d(Q_{ijk}, Q_{ijk}^*) \quad (5.1)$$

where  $n_1$  is the number of image pairs used,  $n_2$  is the number of sets of parameter used for each image pair and  $n_3$  is the total number of voxels of interest.  $i$ ,  $j$  and  $k$  are the indexes of image pair, parameter set and voxels of interest, respectively.  $Q_{ijk}$  and  $Q_{ijk}^*$  correspond to an original voxel of interest  $P_{ijk}$  and they are computed by applying  $T$  and  $T^*$  to  $P_{ijk}$ , respectively. Function  $d$  is the Euclidean distance.



(a) Registration



(b) Mean Displacement Calculation

Figure 5.1: Calculation of the mean displacement

In the experiment, 20 pairs of CT-PET are used and 10 sets of randomly generated parameters within reasonable interval are applied to each pair, i.e.,  $n_1$  and  $n_2$  are equal to 20 and 10, respectively. Three resolution levels including 2mm, 4mm and 8mm are tested for all the 20 image pairs. For each resolution level, mean displacement error for voxels of interest is then computed for each image pair according to Eq. 5.1.

## 5.3 Registration Result

### 5.3.1 Mosaic Images

In this part, we intend to show the capability of the proposed measure in registering images from multiple modalities. In Fig. 5.2 columns (a) and (b), two pairs of CT and PET images from the first dataset, with randomly generated transformation applied to the PET images, are given and the mosaic images before registration is given in columns (c), where contours from CT images are plotted onto the corresponding PET images to show the mis-registration. In column (d) of Fig. 5.2, the mosaic images after registration by the proposed combined mutual information are given.

In Fig. 5.3 and Fig. 5.4 columns (a) and (b), two pairs of CT and PET images from the other two datasets are given and the mosaic images before registration is given in columns (c), where contours from CT images are plotted onto the corresponding PET images to show the mis-registration. In column (d) of these two figures, the mosaic images after registration by the proposed combined mutual information are given. PET images in column (c) and (d) of these two figures are enhanced for better visual effect

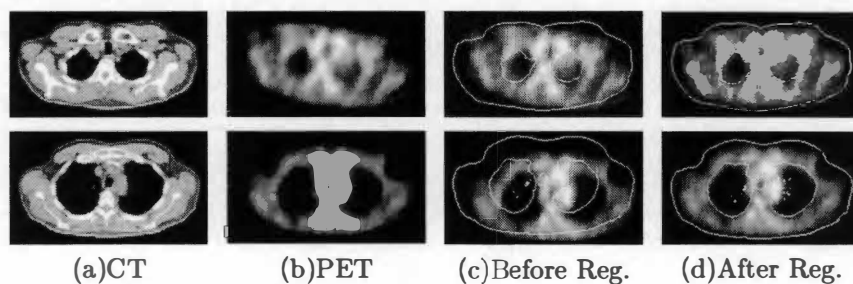


Figure 5.2: Two pairs of CT/PET images from the first dataset and registration result by the combined mutual information

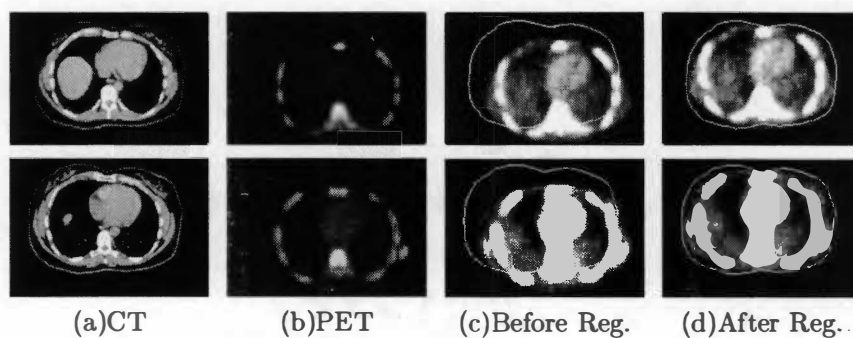


Figure 5.3: Two pairs of CT/PET images from the second dataset and registration result by the combined mutual information

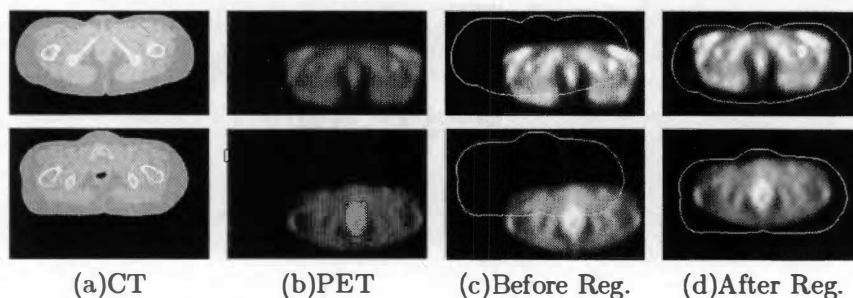


Figure 5.4: Two pairs of CT/PET images from the third dataset and registration result by the combined mutual information



by the means of contrast adjustment.

From the above figures, we can see the combined mutual information successfully registers all the six pairs, where the first two pairs are co-registered and the others are not. Note in Fig. 5.4, because of the existence of fat layer in the imaged subject, the boundaries of the CT and PET images are different. The fat layer is actually absent in the PET images. However, the proposed method succeeds in registering these images.

### 5.3.2 Registration Accuracy Study

In the first part of the performance study, accuracy of these measures is studied. CT and PET images from the first dataset are used in this part. The maximum of the registration measure is assumed to correspond to the true solution; unfortunately, this is only an assumption and it is not always the truth. The purpose is to show how accurate the maximum of a measure corresponds to the correct registration solution. To this end, no transformation is applied to the PET images and registration starts the optimization from the position where the images are registered. In this way, the dependence of the results on the optimization method is minimized. If the maximum of the registration measure coincides with the true solution, the search will find the true solution and the corresponding mean displacement will be minimized, while if that is not true, the search will not find the true solution and the mean displacement will be large. The results therefore indicate how good the maximum of a measure corresponds to the true solution parameters. All five measures are used to optimize the registration. Mean and maximum displacement of voxels of interest for all the 20 image pairs are

Table 5.4: Registration error for accuracy study (In mm)

Measure	Mean Displacement			Max. Displacement		
	8mm	4mm	2mm	8mm	4mm	2mm
$I$	7.19	5.73	5.90	19.19	9.65	16.01
$I_g$	13.39	9.76	6.73	30.91	26.67	14.49
$I_p$	4.65	2.99	2.94	12.57	4.00	16.28
$I_l$	8.24	7.32	4.47	19.20	26.38	16.02
$I_c$	6.60	4.35	2.47	22.37	12.53	4.94

recorded and given in Table 5.4. Three resolution levels including 8mm, 4mm and 2mm are studied.

In the table, at all the three levels,  $I_c$  and  $I_p$  produces lower mean displacements than  $I$  and  $I_g$ ;  $I$  gives better results than  $I_g$  for all resolutions. While for  $I_l$ , it produces better results at 2mm resolution than  $I$  and in all resolutions than  $I_g$ . When comparing all the measures,  $I_c$  gets the best result for 2mm resolution and  $I_p$  is the best for the 8mm and 4mm resolutions. If divide the five measures into two categories, say  $I$  and  $I_g$  of individual measures versus  $I_p$ ,  $I_l$  and  $I_c$  of combining measures and pick the best result in each group, we see the combining measures outperform the single measures at all the three resolutions.

### 5.3.3 Registration Robustness Study

In the second part of the performance study, robustness of these measures is studied. CT and PET images from the first dataset are also used in this study. In this experiment, randomly generated transformation parameters are applied to the test PET images

before the registration. Then the Powell's optimization starts to maximize all the five measures one at a time beginning from where the transformation parameters are all zeros. As local maxima usually exist in the registration function and if that does happen, the optimization will get stuck in those local maxima before they can reach to the global maximum that corresponds to the true solution. However, if a registration measure produces less local maxima, the search algorithm will have better chance to find the true solution and this measure is therefore more robust.

### Comparison of $I$ , $I_g$ and $I_c$

In this comparison, we compare the performance of the combined mutual information with the intensity mutual information and gradient mutual information. Ten sets of randomly generated parameters are used to transform the PET images before registration. In Fig. 5.5, Fig. 5.6 and Fig. 5.7, mean displacements of  $I$ ,  $I_g$  and  $I_c$  for the 20 pairs at resolution of 8mm, 4mm and 2mm are plotted, respectively.

It can be seen that at 4mm resolution  $I_c$  produces superior results for almost all the image pairs compared to  $I$  and  $I_g$ . At 8mm and 2mm the superior of  $I_c$  over  $I$  is not so prominent. At all three resolutions,  $I_c$  produces relatively smooth results for all image pairs, while  $I$  and  $I_g$  gives very big registration error for some images.

### Comparison of All Measures

In Table 5.5, numerical values of the mean and maximum displacements for the 20 pairs of images at all three resolutions are given. From the table, it can be seen that

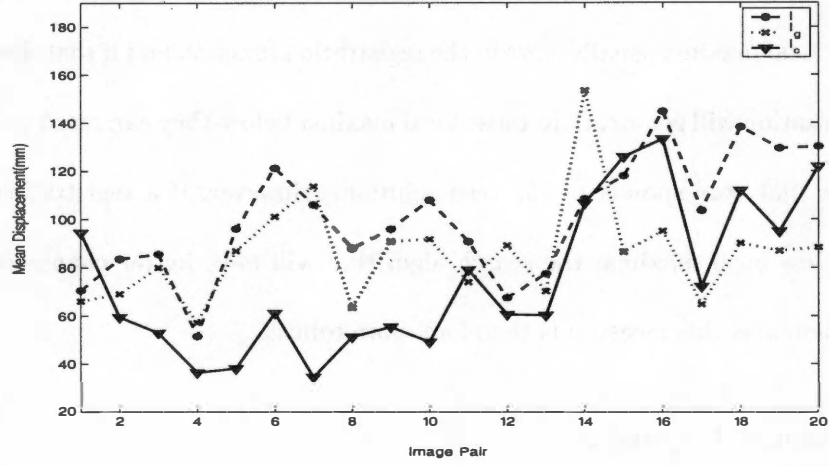


Figure 5.5: Mean displacements of  $I$ ,  $I_g$  and  $I_c$  for 20 image pairs at 8mm resolution

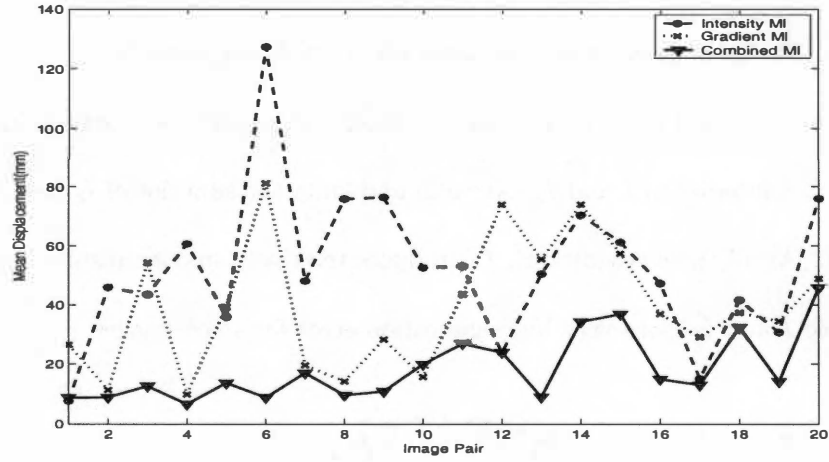


Figure 5.6: Mean displacements of  $I$ ,  $I_g$  and  $I_c$  for 20 image pairs at 4mm resolution

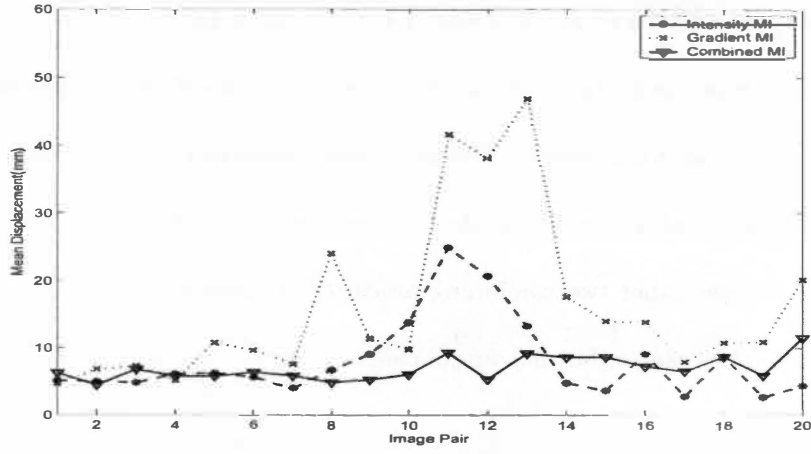


Figure 5.7: Mean displacements of  $I$ ,  $I_g$  and  $I_c$  for 20 image pairs at 2mm resolution

Table 5.5: Registration error for robustness study (In mm)

Measure	Mean Disp.			Max. Disp.		
	8mm	4mm	2mm	8mm	4mm	2mm
$I$	100.74	52.14	8.06	144.74	127.31	24.79
$I_g$	85.93	39.52	15.91	153.47	81.05	46.96
$I_p$	90.90	29.46	12.12	140.70	73.77	40.99
$I_l$	110.21	35.67	7.72	156.39	74.95	21.83
$I_c$	74.97	18.36	6.90	133.23	45.72	11.52

as the resolution gets finer, all measures produces better results by giving lower mean displacement and hence at the finest resolution of 2mm, all measures give the best results. Comparing to the results in Table 5.4, the error in Table 5.5 is much bigger in all resolutions, which indicates that the measures produce local maxima corresponding to mis-registration and the optimization gets stuck into those local maxima before it can reach to the global maximum. In the five measures,  $I_c$  produces the best results at all resolutions. The other two combining measures produce improvements comparing to the individual measures, but not for all cases.

## 5.4 Summary

From the results presented, the gradient mutual information measure  $I_g$  does not produce improvement to the intensity mutual information measure  $I$ . This is not surprised because a lot of intensity information is discarded by only using the spatial information in images.

The combined measure  $I_c$  is able to register CT and PET images and it has produced improvements to the individual measures. The improvements lie in two facets. One is that  $I_c$  is more accurate than the intensity mutual information  $I$  and gradient mutual information  $I_g$  at all resolutions, which means the maximum of  $I_c$  is more accurate than  $I$  and  $I_g$  to indicate the true solution. The other one is  $I_c$  is hence more robust than  $I$  and  $I_g$  at all three resolutions. A direct indication of the improvement is that it might be better to use  $I_c$  in a multi-resolution registration scheme [45][35].

In the three combining measures  $I_p$ ,  $I_l$  and  $I_c$ , the proposed combined measure  $I_c$  produces better results than the other two measures regarding to accuracy at the highest resolution and is the best regarding to robustness at all three resolutions. At coarser resolutions, accuracy of the  $I_c$  is not as good as  $I_p$ . For all the measures, it is possible to reduce the artifacts and hence improve their performance by using other interpolation or histogram estimation methods [46][5], however. Furthermore, we see from the results presented that the combined measures as a whole outperform the individual measures at all resolutions regarding to accuracy and robustness. A conclusion might therefore be drawn that the individual measures could be improved by integrating additional information.

## Chapter 6

# Conclusion

In this thesis, we have studied multi-modal medical image registration by optimizing registration measures based on mutual information of images. Medical image registration methods are first reviewed with a preference to voxel similarity-based methods. We have discussed the mutual information of intensity for image registration with its limitation illustrated. We then proposed a combined mutual information of intensity and gradient, which is a generalization of the intensity mutual information and gradient mutual information. Maximizing the combined mutual information is assumed to correspond to the correct transformation between an image pair.

Optimization methods have been briefly reviewed with the Powell's method discussed in detail. We have chosen to implement the Powell's optimization method. Using this method to optimize the proposed combined mutual information is proven to be an efficient technique to register medical images from multiple modalities.



We have registered slice images scanned in a single patient in the same or different scanning sessions by the proposed combined mutual information. Then we have used 20 pairs of co-registered CT and PET slice images at three different resolutions to study the performance of the proposed measure. Registration of CT and PET images by the use of proposed combined mutual information is compared with the individual mutual information-based registration methods. The proposed method is also compared with the two intensity and gradient combination methods. Experiment results indicate that the proposed combined mutual information produces reliable registrations and it outperforms the intensity- and gradient-based measures at all three resolutions. Among all the three combining measures, the proposed combined measure is the best at the highest resolution regarding to accuracy and better than the other two measures at all resolutions regarding to robustness.

Some future work could be performed beyond to the scope of this thesis. One is to extend the proposed method for three dimensional volume image registration. Though we should expect similar results for volume images, it needs some work to finish the extension. To this end, we have to add three more directions, if rigid body transformation model is used, to the search space, which undoubtedly increases the complexity of the optimization process. We need to give special consideration to interpolation, because the voxel resolution of transaxial slices is often much bigger than in-slice voxel resolution. Both issues are related to implementation to some extent, but they indeed add some uncertainty to the performance of the proposed method for volume image

registration.

Another topic is to investigate some other feature spaces, on which mutual information is to be defined. In this thesis, we discussed mutual information defined on intensity, gradient, and combined space. It is possible to find more efficient feature spaces, however. By defining mutual information on those feature spaces, hopefully we can further improve the performance of the registration measure.

## Bibliography

# Bibliography

- [1] J. Aczel and Z. Daroczy. *On Measures of Information and Their Characterizations*. New York: Academic, 1975.
- [2] T. Beyer, D. W. Townsend, and T. M. Blodgett. Dual-modality pet/ct tomography for clinical oncology. *The quarterly journal of nuclear medicine*, 46(1):24–34, March 2002.
- [3] T. Butz and J. P. Thiran. Affine registration with feature space mutual information. In *Proc. Medical Image Computing and Computer Assisted Intervention (MICCAI'01)*, pages 549–556, Utrecht, The Netherlands, 2001.
- [4] T. Butz and J. P. Thiran. Feature-space mutual information for multi-modal signal processing with application to medical image registration. In *Proc. 11th European Signal Processing Conf. (EUSIPCO'02)*, pages 3–10, Toulouse, France, 2002.
- [5] H. Chen and P. K. Varshney. Mutual information-based *CT-MR* brain image registration using generalized partial volume joint histogram estimation. *IEEE Trans. on Medical Imaging*, 22(9):1111–1119, 2003.

- [6] A. Collignon, F. Maes, D. Delaere, D. Vandermeulen, and P. Suetens. Automated multimodality medical image registration using information theory. In Y. Bizais, C. Barillot, and R. Di Paola, editors, *Computational Imaging and Vision*, volume 3 of *Proc. 14th Int. Conf. Information Processing in Medical Imaging (IPMI'95)*, pages 263–274, Ile de Berder, France, June 1995.
- [7] A. Collignon, D. Vandermeulen, P. Suetens, and G. Marchal. 3D multimodal medical image registration using feature space clustering. In N. Ayache, editor, *in Computer Vision, Virtual Reality, and Robotics in Medicine*, volume 905, pages 195–204. Germany: Springer-Verlag, 1995.
- [8] T. M. Cover and J. A. Thomas. *Elements of Information Theory*. NY: Wiley, New York, 1991.
- [9] K. P. Gall and L. J. Verhey. Computer-assisted positioning of radiotherapy patients using implanted radioopaque fiducials. *Medical Physics*, 20(4):1152–1159, 1993.
- [10] Y. Ge, J. M. Fitzpatrick, J. R. Votaw, S. Gadamsetty, R. J. Maciunas, R. M. Kessler, and R. A. Margolin. Retrospective registration of *PET* and *MR* brain images: an algorithm and its stereotactic validation. *Computer Assisted Tomography*, 18(5):800–810, 1994.
- [11] D. J. Hawkes, D. L. G. Hill, and E. C. M. L. Bracey. Multi-modal data fusion to combine anatomical and physiological information in the head and heart. In

- J. H. C. Reiber and E. E. van der Wall, editors, *Cardiovascular Nuclear Medicine and MRI*, pages 113–130. Kluwer, Dordrecht, The Netherlands, 1992.
- [12] D. L. G. Hill and D. J. Hawkes. Cross-modal registration using intensity-based cost function. In I. N. Bankman, editor, *Handbook of Medical Imaging, Processing and Analysis*, pages 537–554. Academic Pres, 2000.
- [13] D. L. G. Hill, C. Studholme, and D. J. Hawkes. Voxel similarity measures for automated image registration. In R. A. Robb, editor, *Visualization in Biomedical Computing*, volume 2359, pages 205–216. SPIE, 1994.
- [14] M. Holden, D. L. G. Hill, E. R. E. Denton, J. M. Jarosz, T. C. Cox, T. Rohlfing, J. Goodey, and D. J. Hawkes. Voxel similarity measures for 3D serial MR brain image registration. *IEEE Trans. on Medical Imaging*, 19(2):94–102, 2000.
- [15] W. M. Wells III, P. Viola, H. Atsumi, S. Nakajima, and R. Kikinis. Multi-modal volume registration by maximization of mutual information. *Medical Image Analysis*, 1(1):35–51, 1996.
- [16] M. Jenkinson and S. Smith. A global optimisation method for robust affine registration of brain images. *Medical Image Analysis*, 5(2):143–156, 2001.
- [17] H. Jiang, R. A. Robb, and K. S. Holton. A new approach to 3D registration of multimodality medical images by surface matching. In *Visualization in Biomedical Computing*, volume 1808, pages 196–213. SPIE, Bellingham, WA, 1992.

- [18] G. C. Kagadis, K. K. Delibasis, G. K. Matsopoulos, N. A. Mouravliansky, and P. A. Asvestas. A comparative study of surface- and volume-based techniques for the automatic registration between *CT* and *SPECT* brain images. *Medical Physics*, 29(2):201–213, 2002.
- [19] L. V. Laitinen, B. Liliequist, M. Fagerlund, and A. T. Eriksson. An adapter for computer tomography guided stereotaxis. *Surgical Neurology*, 23:559–566, 1985.
- [20] L. Lemieux and R. Jagoe. Effect of fiducial marker localization on stereotactic target coordinate calculation in *CT* slices and radiographs. *Physics in Medicine and Biology*, 39(11):1915–1928, November 1994.
- [21] D. N. Levin, C. A. Pelizzari, G. T. Y. Chen, C. T. Chen, and M. D. Cooper. Retrospective geometric correlation of *MR*, *CT* and *PET* images. *Radiology*, 169(3):817–823, 1988.
- [22] H. Li, B. S. Manjunath, and S. K. Mitra. A contour-based approach to multisensor image registration. *IEEE Trans. on Image Processing*, 4(3):320–334, 1995.
- [23] R. Lundqvist, E. Bengtsson, and L. Thurfjell. A combined intensity and gradient-based similarity criterion for interindividual *SPECT* brain scan registration. *EURASIP Journal on applied signal processing*, 2003(5):461–469, 2003.
- [24] L. D. Lunsfor, editor. *Modern Stereotactic Neurosurgery*. Martinus Nijhoff, 1988.

- [25] F. Maes, A. Collignon, D. Vandermeulen, G. Marchal, and P. Suetens. Multi-modal image registration by maximization of mutual information. *IEEE Trans. on Medical Imaging*, 16(2):187–198, 1997.
- [26] J. B. A. Maintz, P. A. van den Elsen, and M. A. Viergever. Comparison of edge-based and ridge-based registration of *CT* and *MR* brain images. *Medical Image Analysis*, 1(2):151–161, 1996.
- [27] J. B. A. Maintz, P. A. van den Elsen, and M. A. Viergever. Evaluation of ridge seeking operators for multimodal medical image matching. *IEEE Trans. on Pattern Analysis and Machine Intelligence*, 18(4):353–365, 1996.
- [28] J. B. A. Maintz and M. A. Viergever. A survey of medical image registration. *Medical Image Analysis*, 2(1):1–36, 1998.
- [29] P. Neelin, J. Crossinan, D. J. Hawkes, Y. Ma, and A. C. Evans. Validation of an *MRI/PET* landmark registration method using 3D simulated pet images and point simulations. *Computerized medical imaging and graphics*, 17(4-5):351–356, 1993.
- [30] C. A. Pelizzari, G. T. Y. Chen, D. R. Spelbring, R. P. Weichselbaum, and C. T. Chen. Accurate three-dimensional registration of *CT*, *PET*, and/or *MR* images of the brain. *Computer Assisted Tomography*, 13:20–26, 1989.



- [31] G. P. Penney, J. Weese, J. A. Little, P. Desmedt, D. L. G. Hill, and D. J. Hawkes. A comparison of similarity measures for use in 2D-3D medical image registration. *IEEE Trans. on Medical Imaging*, 17(4):586–595, 1999.
- [32] U. Pietrzyk, K. Herholz, G. Fink, A. Jacobs, R. Mielke, I. Slansky, M. Wurker, and W. Heiss. An interactive technique for three-dimensional image registration: validation for *PET*, *SPECT*, *MRI* and *CT* brain studies. *The Journal of Nuclear Medicine*, 35(12):2011–2018, 1994.
- [33] D. Plattard, M. Soret, J. Troccaz, P. Vassal, J.-Y. Giraud, G. Champleboux, X. Artignan, and M. Bolla. Patient setup using portal images: 2D/2D image registration using mutual information. *Computer Aided Surgery*, 5(4):246–262, 2000.
- [34] J. P. W. Pluim, J. B. A. Maintz, and M. A. Viergever. Image registration by maximization of combined mutual information and gradient information. *IEEE Trans. on Medical Imaging*, 19(8):809–814, 2000.
- [35] J. P. W. Pluim, J. B. A. Maintz, and M. A. Viergever. Mutual information matching in multiresolution contexts. *Image and Vision Computing*, 19:45–52, 2001.
- [36] J. P. W. Pluim, J. B. A. Maintz, and M. A. Viergever. Mutual-information-based registration of medical images: a survey. *IEEE Trans. on Medical Imaging*, 22(8):986–1004, 2003.
- [37] W. H. Press, B. P. Flannery, S. A. Teukolsky, and W. T. Vetterling. *Numerical recipes in C*. Cambridge Univ. Press, Cambridge, U. K., 1992.

- [38] A. Rangarajan, H. Chui, and J. S. Duncan. Rigid point feature registration using mutual information. *Medical Image Analysis*, 3(4):425–440, 1999.
- [39] N. Ritter, R. Owens, J. Cooper, R. H. Eikelboom, and P. P. van Saarloos. Registration of stereo and temporal images of the retina. *IEEE Trans. on Medical Imaging*, 18(5):404–418, 1999.
- [40] A. Roche, G. Malandain, X. Pennec, and N. Ayache. The correlation ratio as a new similarity measure for multimodal image registration. In *Proc. MICCAI'98*, pages 1115–1124, Cambridge, Massachusetts, October 1998.
- [41] L. R. Schad, R. Boesecke, W. Schlegel, G. H. Hartmann, G. H. Sturm, L. G. Strauss, and W.J. Lorenz. Three dimensional image correlation of *CT*, *MR*, and *PET* studies in radiotherapy treatment of brain tumors. *Computer Assisted Tomography*, 11:948–951, 1987.
- [42] C. Studholme, D. L. G. Hill, and D. J. Hawkes. Multiresolution voxel similarity measures for *MR-PET* registration. In Y. Bizais, C. Barillot, and R. Di Paola, editors, *Proc. of Information Processing in Medical Imaging*, pages 287–298, Brest, France, 1995. Kluwer Academic Publishers.
- [43] C. Studholme, D. L. G. Hill, and D. J. Hawkes. An overlap invariant entropy measure of 3D medical image alignment. *Pattern Recognition*, 32(1):71–86, 1999.
- [44] J. West *et al.* Comparison and evaluation of retrospective intermodal image registration techniques. *Journal of Computer Assisted Tomography*, 21:554–566, 1997.

- [45] P. Thevenaz and M. Unser. Optimization of mutual information for multiresolution image registration. *IEEE Trans. on Image Processing*, 9(12):2083–2099, 2000.
- [46] J. Tsao. Interpolation artifacts in multimodal image registration based on maximization of mutual information. *IEEE Trans. on Medical Imaging*, 22(7):854–864, 2003.
- [47] P. A. van den Elsen, J. B. A. Maintz, E-J. D. Pol, and M. A. Viergever. Automatic registration of *CT* and *MR* brain images using correlation of geometrical features. *IEEE Trans. on Medical Imaging*, 14(2), 1995.
- [48] P. A. van den Elsen, E-J. D. Pol, and M. A. Viergever. Medical image matching-a review with classification. *IEEE Engineering in Medicine and Biology*, 12(1):26–39, 1993.
- [49] M. van Herk and H. M. Kooy. Automatic three-dimensional correlation of *CT-CT*, *CT-MRI*, and *CT-SPECT* using chamfer matching. *Medical Physics*, 21(7):1163–1177, 1994.
- [50] M. A. Viergever, J. B. A. Maintz, and R. Stokking. Integration of functional and anatomical brain images. *Biophysical Chemistry*, 68(1-3):207–219, 1997.
- [51] M. Y. Wang, J. M. Fitzpatrick, and C. R. Maure. Design of fiducials for accurate registration of *CT* and *MR* volume images. In M. Loew, editor, *Medical Imaging*, volume 2434, pages 96–108. SPIE, 1995.

- [52] M. Y. Wang, C. R. Maurer, J. M. Fitzpatrick, and R. J. Maciunas. An automatic technique for finding and localizing externally attached markers in *CT* and *MR* volume images of the head. *IEEE Trans. on Biomedical Engineering*, 43(6):627–637, June 1996.
- [53] R. P. Woods. Spatial transform models. In I. N. Bankman, editor, *Handbook of Medical Imaging*, pages 465–490. Academic Press, 2000.
- [54] R. P. Woods, J. C. Mazziotta, and S. R. Cherry. *MRI-PET* registration with automated algorithm. *Computer Assisted Tomography*, 17(4):536–546, July/Aug. 1993.

## **Vita**

Wei Jiang was born in Sichuan, P.R. China on June 15, 1977. After graduation from Nanchong High School in 1996, he attended Sichuan University and graduated in 2000 with a Bachelor of Science degree in Electrical Engineering. Upon graduation from Sichuan University, he entered Sichuan University Graduate School with the major in Electrical Engineering. In fall 2002, he was awarded a graduate scholarship from the Department of Electrical and Computer Engineering of the University of Tennessee, Knoxville and came to United State to pursue a graduate degree. He worked as a research assistant in the Lab of Dr. Seong G. Kong and a teaching assistant for the ECE department. He will receive a Master of Science degree in Electrical Engineering upon the approval of the thesis.

5990 2949 29  
06/23/04 NFB